B_0-ANGLE EFFECT ON ZONAL AND MERIDIONAL FLOW DETERMINATIONS FROM 3 YEARS RING DIAGRAM ANALYSIS OF GONG++ DATA

A. Zaatri[1,3], R. Komm[2], I. Gonzalez-Hernandez[2], R. Howe[2], and T. Corbard[3]

[1]*Centre de Recherche en Astronomie, Astrophysique et Géophysique, BP 63, Route de l'Observatoire, Bouzaréah, 16340, Algiers, Algeria*
[2]*National Solar Observatory, 950 N, Cherry avenue, Tucson AZ 85719, USA*
[3]*Département Cassiopée, UMR CNRS 6202, Observatoire de la Côte d'Azur, BP 4229, 06304 Nice, CEDEX 4, France*

ABSTRACT

We study zonal and meridional components of horizontal solar subsurface flows during the years 2001-2004 which covers the declining phase of solar cycle 23. We measure the horizontal flows from the near surface layers to $16Mm$ in depth by analyzing 44 consecutive Carrington rotations of Global Oscillation Network Group (GONG) Doppler images with a ring-diagram analysis technique. The meridional flow shows an annual variation related to the B_0-angle variation, while the zonal flow is less affected by this variation. After correcting for this effect, the meridional flow is mainly poleward but it shows a counter cell close to the surface at high latitudes in both hemispheres.

Key words: local helioseismology; horizontal flows; B_0-angle.

1. INTRODUCTION

We use ring diagram analysis of long term high resolution GONG doppler images (1024×1024 pixel array) in order to measure horizontal flow components from the central meridian distance (CMD) to ± 52.5 in latitude, and from the surface to about $16Mm$ in depth. We deduce these components from 3-dimensional power spectra of tracked small patches ($16^\circ \times 16^\circ$) of doppler images using the RLS inversion method. We mainly focus on the systematic effect caused by the B_0-angle in the temporal pattern of meridional and zonal flows. Indeed, the systematic variations of observational origins that might bias the derived flows can be checked for a given length of the data set where magnetic activity has a constant distribution.
Ring diagram analysis takes into account several geometrical effects such as the apparent semi-diameter of the sun and the solar inclination toward the Earth (B_0-angle). However, this procedure cannot correct for a loss in detail that can occur at high spatial frequencies due to this variation. For instance, big rings analysis of GONG data revealed that an equatoward meridional cell appears at high latitudes during maximum values of the B_0-angle and that it appears either in the northern or southern hemisphere depending on the sign of the B_0-angle [5]. In the current work, we correct the measured horizontal flow components from the B_0-angle effect after proving their correlation in some parts of the observed areas, notably, at high latitudes and very close to the surface.

2. DATA ANALYSIS

The data used in this work consists of continuous high resolution Dopplergrams from the Global Oscillation Network Group (GONG) covering 44 consecutive Carrington rotations from CR 1979 to CR 2022 (July 27, 2001 october 12, 2004). Full-disk Dopplergrams at 1 minute cadence are recorded on a 1024×1024 pixel CCD [1] and then registered so that the solar image covers an area of 800 pixel in diameter. We use ring diagram analysis in order to measure the horizontal components of the solar subsurface flows as a function of depth [2]. This technique studies high degree ($\ell > 300$) acoustic waves measured in small patches ($15^\circ \times 15^\circ$) by assuming a wave plane approximation. A set of 189 overlapped patches with centers separated by 7.5° in latitude and longitude covers the solar disk from the central meridian distance (CMD) to $\pm 52.5^\circ$. Each patch is tracked at the surface rotation rate in order to remove the differential rotation effect and appodized with a circular function. These patches are stored in dense-packs of $1664mn$ covering a one GONG day.
3-dimensional power spectra are constructed from each dense pack using the 3-dimensional FFT so that the spatial and temporal coordinates (x, y, t) are substituted by k_x, k_y, ν, where k_x and k_y are the components of the horizontal wave number and ν is the temporal frequency.
Level sets of the power spectrum at specified frequencies give 'rings' which are shifted by velocity flows. Using this notion, the power spectrum is fitted via a Lorentzian profile model which incorporates a perturbance term, $k_x\ v_x + k_y\ v_y$, due to the horizontal velocity flows [**?**]. Finally, the Regularized Least Square (RLS) method

is used to invert velocities calculated from the fitting process to horizontal velocity flow components as functions of depth $(v_x(r), v_y(r))$, where the components are respectively called zonal and meridional flows [3].
For this work, we average the horizontal flows over the length of a Carrington rotation and study the temporal variation of zonal and meridional flows from more than three years of consecutive GONG data.

3. RESULTS

3.1. Meridional flow variablility

Higher panel of fig.1 shows the long term pattern of the meridional flow at 4 latitudes and 4 depths. Meridional flows are mainly poleward in each hemisphere, except at high latitudes and very close to the surface ($52.5°$ and $0.6Mm$) where flows are equatorward (counter cell) in both hemispheres. At high latitudes and low depths, these meridional flows exhibit periodic trends recurring on a yearly basis. This periodic variation seems to be well correlated with that of the B_0-angle in these regions. This correlation is shown by linear regression of the flow with the B_0-angle included on the same chart. Moreover, correlation coefficients shown in fig.2 at the same latitudes and depths show overall a good correlation between the B_0-angle and flow variabilities. Large correlation coefficients occur mainly at high latitudes, while the values are generally small close to the equator. The correlation values are very similar in both hemispheres except at shallow layers equatorward of about $30°$ and at depths greater than about $10Mm$ poleward of about $30°$.

We remove the B_0-angle effect from the meridional flow variability by subtracting the fit of a linear regression between flow and B_0-angle variation (lower panel of fig.1). The 1-year periodicity disappeares. Consequently, one can conclude that such a periodicity is purely a systematic effect due to the B_0-angle. However, the counter cell still appears at high latitudes in shallow layers in both hemispheres.

We calculate the meridional flow averaged over CR 1979–2022 corrected for the B_0-angle variation (fig.3). Steep gradients at latitudes of about $35°$ or $40°$ and higher are shown. At these latitudes, the flow amplitudes decrease with increasing latitude at shallow depths (below about $2Mm$), while they increase with latitude at greater depths and then decrease again at depths greater than about $13Mm$ (not shown). The counter cell is noticeable close to the surface at the highest latitudes.

3.2. Zonal flow variablility

Higher panel of fig.4 shows the long term pattern of the zonal flow at 4 latitudes and 4 depths. As for the meridional flow variability, we incorporate a low-degree polynomial fit of the flow with the B_0-angle for the 16 panels.

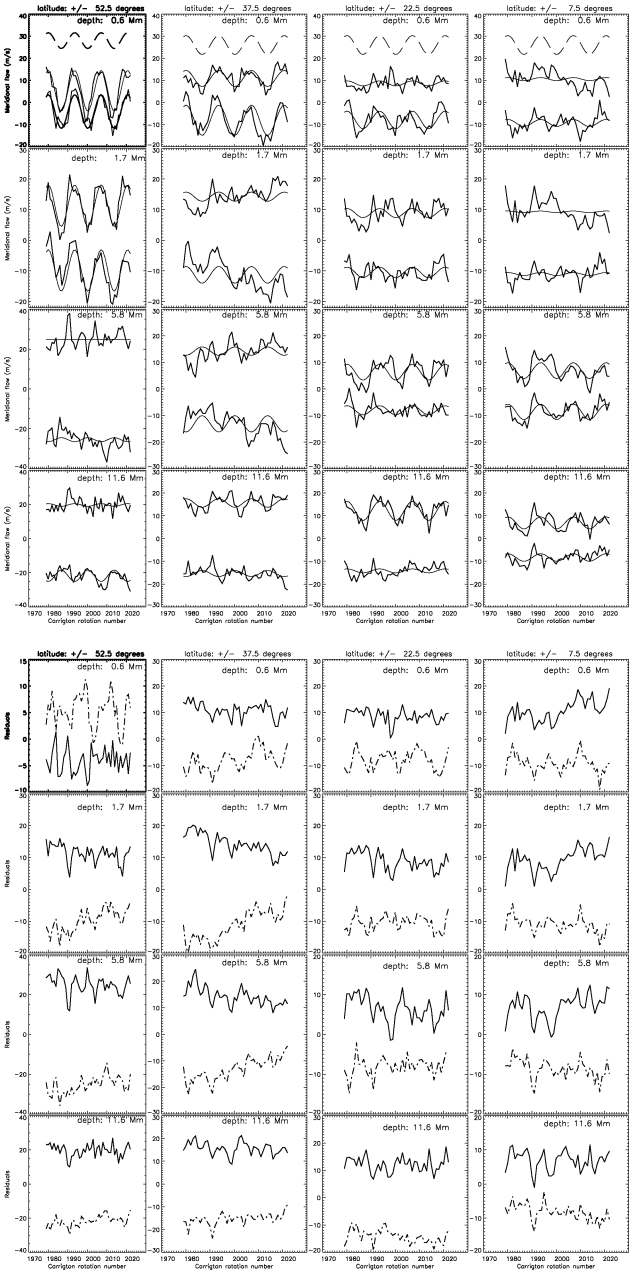

Figure 1. Top:Temporal variation of the meridional flow in the northern (full-black) and southern hemisphere (dotted-red). The B_0-angle variation (in degree) is indicated as dashed line in the top row (shifted by $30m/s$ in the y-direction). Thin full lines represent linear fits of the B_0-angle to the flows. Bottom: Same as top panel after removing the B_0-angle variation from the meridional flow.

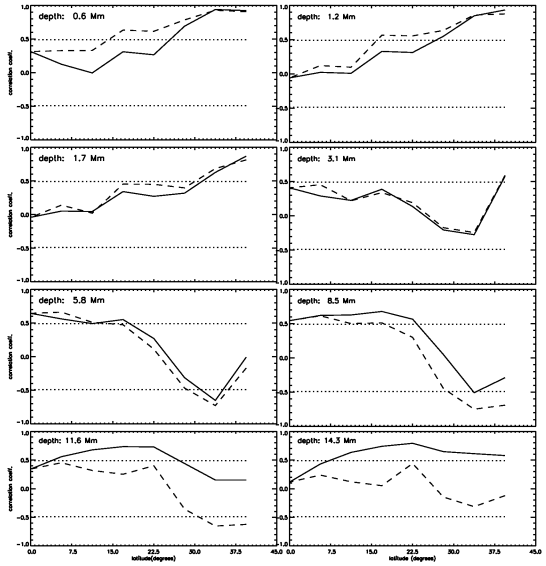

Figure 2. Linear correlation coefficient between meridional flow and B_0-angle variation. The dotted lines indicate the 99.9 % significance levels.

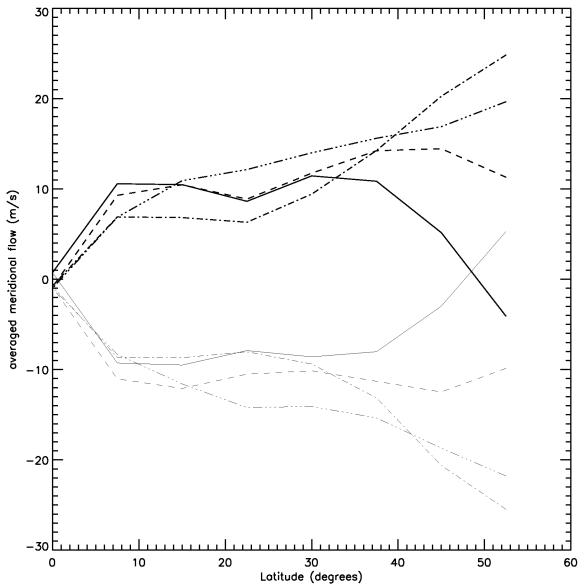

Figure 3. Averaged meridional flow as a function of latitude at four different depths (0.6 Mm: solid, 1.7 Mm: dashed, 5.8 Mm: dot-dashed, 11.6 Mm: 3dot-dashed) for the northern (black) and the southern hemisphere (red).

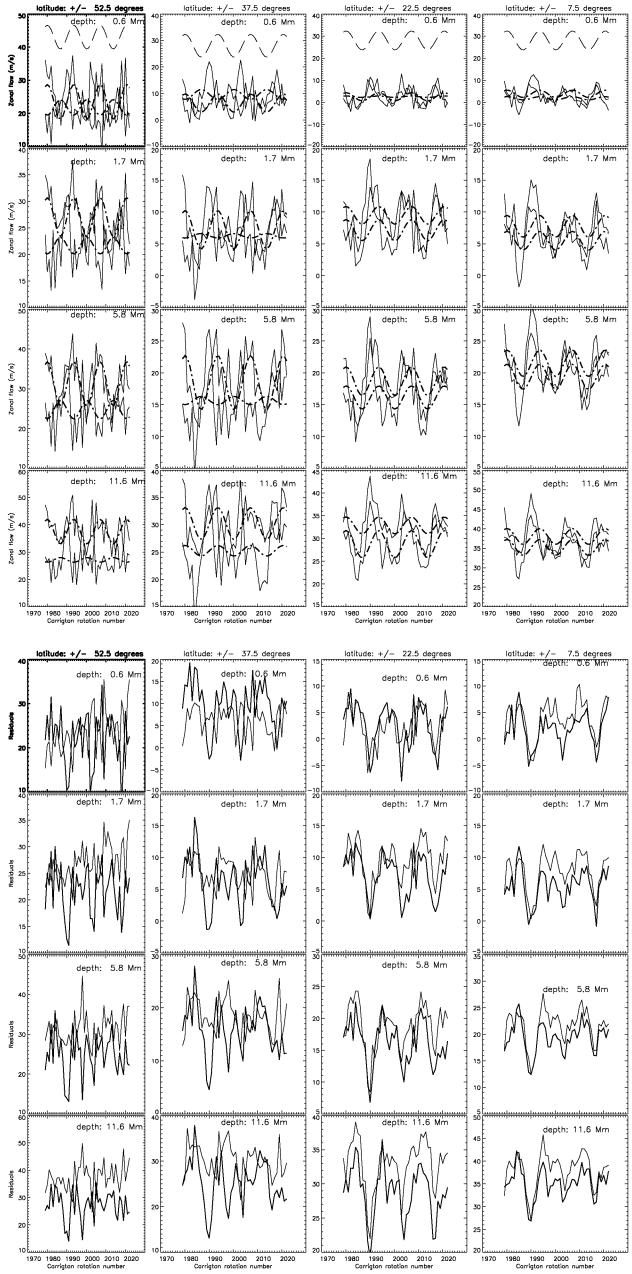

Figure 4. Top:Temporal variation of the zonal flow in the northern (full-black) and southern hemisphere (full-red). The B_0-angle variation (in degree) is indicated as dashed line in the top row (shifted by $30m/s$ in the y-direction). Thin dashed-dotted lines represent linear fits of the B_0-angle to the flows (red: for the southern flow, black: for the northern flow). Bottom: Same as top panel after removing the B_0-angle variation from the zonal flow.

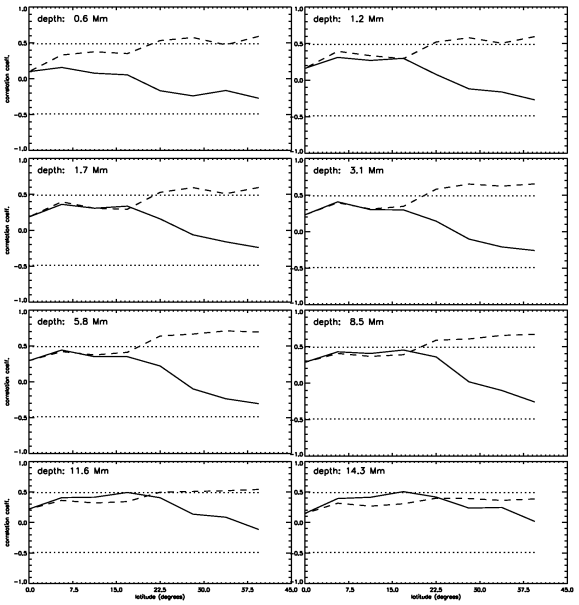

Figure 5. Same as figure 2 for zonal flow

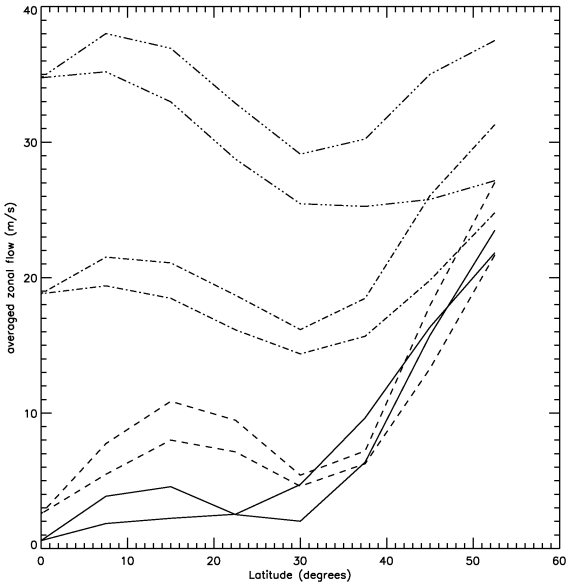

Figure 6. Same as figure 3 for zonal flow

In contrast to meridional flows, the temporal variation of the zonal flow is less correlated with the B_0-angle variation (see fig.5). It is significantly correlated with the B_0-angle only in the southern hemisphere at depths between 2 and 11 Mm. At the same depth range in the northern hemisphere, the correlation is negative and increases in amplitude with increasing latitude but remains below the 99.9% significance level.

In reference [6], we show that the correlation between the zonal flow and the B_0-angle shows the same pattern with latitude and depth as the correlation between the errors of the zonal flow and the B_0- angle. For this reason, we decided to remove the B_0-angle effect from the zonal flow, as shown in the upper panel of fig.4.

The zonal flow shows strong fluctuations on time scales shorter than one year, which appears to be correlated between the hemispheres at 7.5° and 22.5° latitude. At latitudes poleward of about 40°, the variation of the zonal flow appears to have a larger amplitude compared to more equatorward latitudes.

The averaged zonal flow corrected for the B_0-angle variation is shown in Fig.6. It increases in amplitude with increasing depth. The zonal flow is predominantly faster in the southern hemisphere than in the northern one. The differences generally increase with increasing latitude for latitudes greater than 25°. Furthermore, the difference in amplitude between the hemispheres increases with depth with a local maximum near 15° latitude.

4. SUMMARY

We have analyzed 44 consecutive Carrington rotations of Global Oscillation Network Group (GONG) Doppler images with a ring-diagram analysis technique and explored the horizontal flow components and their temporal variation. We mainly focused on the B_0-angle effect on flows variations in time.
The meridional flow pattern is found to be sensitive to the B_0-angle variation in [5]. In fact, the 1 year periodicity which appears especially at high latitudes in shallow layers disappears when the systematic effect caused by the B_0-angle variation in time is removed by subtracting a linear regression in B_0-angle from the flows. However, the presence of the counter cell at high latitudes and low depths does not disappear after removing the B_0-angle effect. Moreover, it's location differs from other studies ([5] and [4], for exemple). Consequently, we can't rule out the possibility that it's due to some systematic effect.
We also show that the averaged meridional flow amplitude over the period of observation has a steep depth gradient at high latitudes. This averaged meridional flow is found to be more poleward in the south at higher depths for all latitudes.
In contrast, the zonal flow variability is not affected by the B_0-angle variation in time. The averaged amplitude of the zonal flow over these 44 Carrington rotation is predominant in the southern hemisphere.
The meridional and zonal flow patterns are strongly related to the solar cycle variability and hence to the magnetic flow pattern. In the reference [6], we give further discussion of this view.

REFERENCES

[1] Harvey, J., Tucker, R., & Britanik, L., 1998, *in S.G. Korzennik & A. Wilson (eds.), Structure and Dynamics of the Interior of the Sun and Sun-like Stars, ESA SP-418, Noordwijk: ESA*, 209

[2] Hill, F., 1988 *Astrophys. J.* 339, 996

[3] Corbard, T., Toner, C., Hill, F., Hanna, K.D., Haber, D.A., Hindman, B.W., & Bogard, R.S., 2003, *in H. Sawaya-Lacoste (ed.), Local and Global Helioseismology: The present and Future, ESA* SP-517, Noordwijk: ESA, 255.

[4] Haber D.A., Hindman, B.W., Toomre, J., Bogart, R.S., Larsen, R.M., & Hill, F., 2002, *Astrophys. J.* 570, 885

[5] Gonzalez Hernandez, I., Komm, R., Hill, F., Howe, R., Corbard, T.,& Haber, D.A., 2006, *Astrophys. J* 638, 576

[6] Zaatri A., Komm R., Gonzalez Hernandez I., Howe R., Corbard T., 2006, *Solar physics* 236, 227